ture.[21,22] In Table II the rates of exchange between the various complexes discussed in this paper are compiled. These rates are based on the experimental data presented in Figures 1, 3, and 8. Most frequently upper limits only of exchange rates can be calculated. Whenever the different observed nuclei give different upper limits, the lowest of these is the closest to the actual rate. Therefore, the hydrated aluminum exchanges with complex I at a rate slower than 1100 s^{-1}, and complexes III and IV have a rate between them smaller than 130 s^{-1}. Likewise, structures a and b within complex III exchange at a rate slower than 90 s^{-1}. In two cases, between complex I and complex II and also between complex II and complex III, both a lower and an upper limit are available. The ability, in these cases, to obtain both limits is due to the fortunate coincidence of two different NMR nuclei having chemical shift differences such that one happens to be in slow and the other in fast exchange relative to their reference rates. Therefore, the actual chemical exchange rates become revealed due to this bracketing. These are ~65 s^{-1} for the exchange between complexes I and II and 1000 s^{-1} for complexes II and III.

(21) Pople, J.; Schneider, W. G.; Bernstein, H. J. "High Resolution Nuclear Magnetic Resonance"; McGraw Hill: New York, 1959.
(22) Swift, T. J.; Connick, R. E. *J. Chem. Phys.* **1962**, *37*, 307.

Acknowledgment. We thank Dr. R. P. Pillai for a critical reading of the manuscript and Dr. Peter Roller for letting us use his NMR instrument while ours was out of order.

Simulation of Reaction Pathways in Enzymatic and Nonenzymatic Hydrolysis of *p*-Nitrophenyldeoxythymidine Diphosphate

Joan A. Deiters[1a] and Robert R. Holmes*[1b]

Contribution from the Departments of Chemistry, University of Massachusetts, Amherst, Massachusetts 01003, and Vassar College, Poughkeepsie, New York 12601.
Received May 10, 1982

Abstract: A computer model, based on a molecular mechanics approach, is developed for the hydrolysis of the substrate *p*-nitrophenyldeoxythymidine diphosphate, *p*-NO_2Ph-pdTp, in the enzyme system Ca^{2+}–staphylococcal nuclease. The model is based on X-ray data (1.5-Å resolution) for the enzyme substrate system Ca^{2+}–staphylococcal nuclease–pdTp, where pdTp represents deoxythymidine diphosphate. Calcium–oxygen interactions and hydrogen bonding are included in the model to mimic enzyme–substrate interaction. The energy profiles of two hydrolysis pathways are investigated: path 1, an attack at phosphorus in line with OR where R = *p*-NO_2Ph, leads to the products observed experimentally in nonenzymatic hydrolysis; path 2, attack at phosphorus in line with OR′ where R′ = deoxythymidine 3′-phosphate, leads to the products observed in enzymatic hydrolysis. The results of the calculation, done under constraints similar to those used for 2.0-Å data, show that in the enzymatic system path 1 is of higher energy unless extensive atomic rearrangement occurs. The higher energy of path 1 results from the fact that attack in line with OR, where R = *p*-NO_2Ph, is blocked by a nitrogen atom of Arg-35. The results calculated from the enzymatic system are compared also with the earlier calculation on nonenzymatic hydrolysis of *p*-NO_2Ph-pdTp.

Introduction

Possible mechanisms for the action of the enzyme staphylococcal nuclease–Ca^{2+} in phosphate hydrolysis have been proposed[2,3] based on experimental data giving structural information for the active site. These data have been based on NMR investigations utilizing paramagnetic probes[4] and single-crystal X-ray diffraction studies.[3b,5,6] In a previous paper[7] using atomic coordinates from X-ray diffraction studies,[5,8,9] the methods of molecular mechanics were applied to give a computer simulation of the energy profile for enzymatic and nonenzymatic hydrolysis of the substrate *p*-nitrophenyl-pdTp where pdTp is deoxythymidine diphosphate. The initial conformation of the substrate *p*-nitrophenyl-pdTp in the active site of the enzyme, staphylococcal nuclease–Ca^{2+}, was obtained by modifying the X-ray coordinates of 2.0-Å resolution for the inhibitor–enzyme complex, pdTp–Ca^{2+}–staphylococcal nuclease. When a further refinement of the X-ray data to 1.5-Å resolution showed that there was considerable change in the active site,[3b] particularly in the region immediately surrounding the calcium ion, we wished to see how these changes in atomic coordinates affected the energy profile of possible hydrolysis reaction pathways and also whether or not there were high-energy barriers along the reaction pathway proposed by Cotton and Hazen[3b] based on X-ray data of 1.5-Å resolution. In this present work, the atomic coordinates of 1.5-Å resolution, obtained from the inhibitor–enzyme complex pdTp–Ca^{2+}–staphylococcal nuclease, are used and modified to obtain a minimum energy conformation for the active substrate *p*-nitrophenyl-pdTp in an enzymatic environment. The energy profile of two possible reaction pathways was calculated and compared with earlier results based on 2.0-Å data[7] and

(1) (a) Vassar College. (b) University of Massachusetts.
(2) Anfinsen, C. B.; Cuatrecasas, P.; Taniuchi, H. "The Enzymes", 3rd ed.; Boyer, P. D., Ed.; Academic Press: New York, 1971; Vol. IV, pp 177–204.
(3) (a) Cotton, F. A.; Day, V. W.; Hazen, E. E., Jr.; Larsen, S. *J. Am. Chem. Soc.* **1973**, *95*, 4834. (b) Cotton, F. A.; Hazen, E. E., Jr.; Legg, M. J. *Proc. Natl. Acad. Sci. U.S.A.* **1979**, *76*, 2551.
(4) Furie, B.; Griffen, J. H.; Feldmann, R. J.; Sokoloski, E. A.; Schechter, A. N. *Proc. Natl. Acad. Sci. U.S.A.* **1974**, *71*, 2833.
(5) Arnone, A.; Bier, C. J.; Cotton, F. A.; Day, V. W.; Hazen, E. E., Jr.; Richardson, D. C.; Richardson, J. S.; Yonath, A. *J. Biol. Chem.* **1971**, *246*, 2302.
(6) Arnone, A.; Bier, C. J.; Cotton, F. A.; Hazen, E. E., Jr.; Richardson, D. C.; Richardson, J. S. *Proc. Natl. Acad. Sci. U.S.A.* **1969**, *64*, 420.
(7) Deiters, J. A.; Gallucci, J. C.; Holmes, R. R. *J. Am. Chem. Soc.* **1982**, *104*, 5457.
(8) Trueblood, K. N.; Horn, P.; Luzzati, V. *Acta Crystallogr., Sect. B* **1961**, *14*, 965.
(9) Young, D. W.; Tollin, P.; Wilson, H. R. *Acta Crystallogr., Sect. B* **1969**, *25*, 1423.

0002-7863/83/1505-0609$01.50/0 © 1983 American Chemical Society

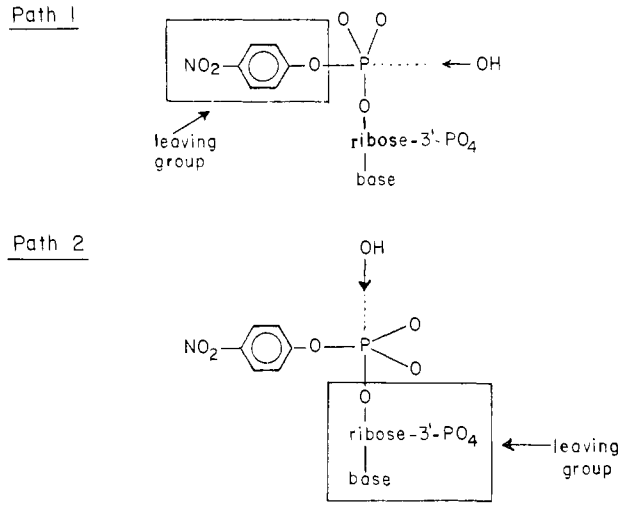

Figure 1. Alternate pathways for nonenzymatic and enzymatic hydrolysis of *p*-NO_2Ph-pdTp.

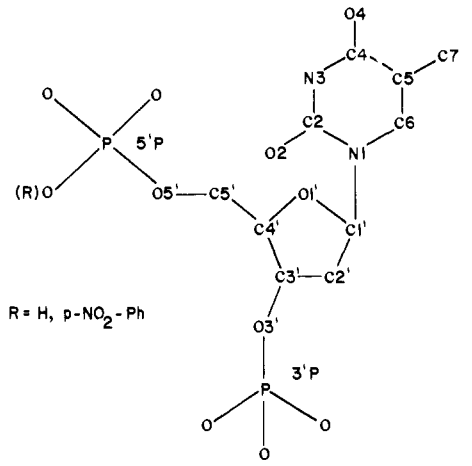

Figure 2. Conventional numbering scheme for pdTp and *p*-NO_2Ph-pdTp where R = *p*-NO_2Ph.

with experimental results for enzymatic and nonenzymatic hydrolysis.[10]

Description of Method

In modeling staphylococcal nuclease action on the active substrate, *p*-NO_2Ph-pdTp, using techniques devised for a molecular mechanics approach to the ribonuclease–UpA system[11,12] and for earlier calculations[7] on Ca^{2+}–*p*-NO_2Ph-pdTp–staphylococcal nuclease (based on 2.0-Å resolution X-ray data),[5] we used atomic coordinates of the 1.5-Å resolution data[2,13] on the nuclease–pdTp–Ca(II) ion system as a starting point. After introduction of active site enzyme fragments and specific enzyme constraints of weak interactions between enzyme and substrate, atomic coordinates were adjusted by the methods of molecular mechanics to obtain a minimum energy conformation. This conformation of the enzyme–inhibitor pdTp was then altered by the addition of a *p*-nitrophenyl group and again minimized to give a minimum energy conformation of the active substrate, *p*-NO_2Ph-pdTp, in the active site environment. Minimum energy conformations were obtained at points along two different reaction pathways by methods described earlier.[7] The two pathways investigated were path 1, attack in line with OR where R = *p*-NO_2Ph (this path leads to the products observed[10] in nonenzymatic hydrolysis); and path 2, attack in line with OR′ where R′ is deoxythymidine 3′-phosphate (this path leads to the products observed[10] in enzymatic hydrolysis). See Figure 1.

Table I. Calculated Energy of pdTp–Ca(II)–Staphylococcal Nuclease System[a]

	atomic coordinates from X-ray data (1.5-Å resolution)	atomic coordinates of minimum energy conformation
ΣE_{str}[b]	721.10	0.63
ΣE_{bend}	51.59	2.40
ΣE_{VDW}[c]	−1.41	−1.89
ΣE_{tors}	8.34	0.70
Σ total	779.62	1.21

[a] All energies are reported in kcal/mol. [b] The energy expression is $E_{steric} = \Sigma E_{str} + \Sigma E_{bend} + \Sigma E_{tors} + \Sigma E_{NB} + \Sigma E_{EPR}$. [c] $\Sigma E_{VDW} = \Sigma E_{NB} + \Sigma E_{EPR}$.

Table II. Conformational Parameters for Substrate pdTp and *p*-NO_2Ph-pdTp in Ca(II)–Staphylococcal Nuclease System

	X-ray coordinates	minimum energy coordinates	
	pdTp	pdTp	*p*-NO_2Ph-pdTp
dihedral angle (deg) between thymine plane and plane of ribose[a]	62.4	63.5	65.0
torsional angles (deg)			
ϕ_{CN} $O_1'C_1'N_1C_2$[b]	156.1	154.3	154.5
$O_1'C_1'N_1C_6$	26.4	28.5	28.3
ϕ_{OO} $O_5'C_5'C_4'O_1'$	50.4	59.2	59.6
ϕ_{OC} $O_5'C_5'C_4'C_3'$	169.0	173.9	175.4
distance (Å) from mean plane 1[c]			
C_3'	0.31	0.35	0.36
C_5'	−1.38	−1.36	−1.34
O_3'	1.58	1.73	1.76
N_1	−1.07	−1.10	−1.09
distance (Å) from mean plane 2[d]			
C_2'	−0.34	−0.31	−0.32
C_5'	−1.41	−1.42	−1.41
O_3'	1.21	1.35	1.38
N	−1.04	−1.07	−1.06

[a] Five atoms included in ribose plane. [b] All atoms numbered as in Figure 2. [c] Mean plane 1 = mean plane of atoms $C_1'C_2'C_4'O_1'$. [d] Mean plane 2 = mean plane of atoms $C_1'C_3'C_4'O_1'$.

Initial Minimum Energy of Enzyme–Inhibitor Complex. From the X-ray coordinates for pdTp–Ca(II)–staphylococcal nuclease[13] certain atomic coordinates were selected to provide a starting point in the establishment of the computer model for the enzyme–substrate system. Selected for inclusion in the model were the inhibitor molecule, pdTp; calcium ion; three water molecules near the active site; enzyme fragments at the active site, namely, Asp-21, Asp-40, Glu-43, Arg-35, Arg-87, Tyr-113, Tyr-85, and Thr-41. These enzyme fragments were selected because they appear to have a role in the binding of pdTp to the active site.[3] The conventional numbering system of pdTp is shown in Figure 2. In our calculations, each atom requires a unique number; the numbering scheme used is shown in Figure 3. All bond length, bond angle, torsional, van der Waals, and electron pair repulsion parameters were the same as those previously described.[7] Parameters for enzyme–substrate interactions are included in Table III and are discussed in a later section.

When the methods of molecular mechanics are applied to atomic coordinates which have been obtained from X-ray data of 1.5-Å resolution, the high strain energy present, due to un-

(10) Dunn, B. M.; DiBello, C.; Anfinsen, C. B. *J. Biol. Chem.* **1973**, *248*, 4769.
(11) Holmes, R. R.; Deiters, J. A.; Gallucci, J. C. *J. Am. Chem. Soc.* **1978**, *100*, 7393.
(12) (a) Deiters, J. A.; Gallucci, J. C.; Clark, T. E.; Holmes, R. R. *J. Am. Chem. Soc.* **1977**, *99*, 5461. (b) Allinger, N. L.; Tribble, M. T.; Miller, M. A.; Wertz, D. H. *Ibid.* **1971**, *93*, 1637. (c) Wertz, D. H.; Allinger, N. L. *Tetrahedron*, **1974**, *30* 1579.
(13) Hazen, E. E., Jr., private communication.

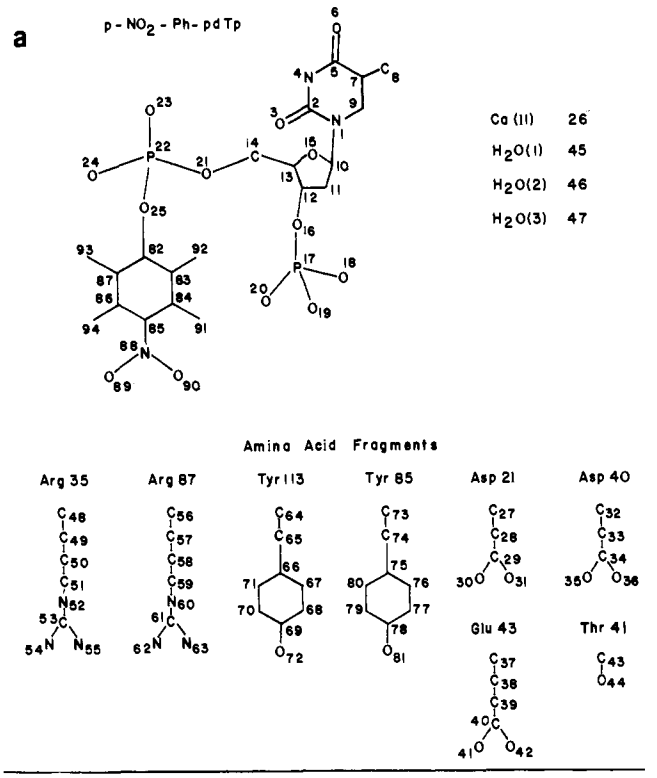

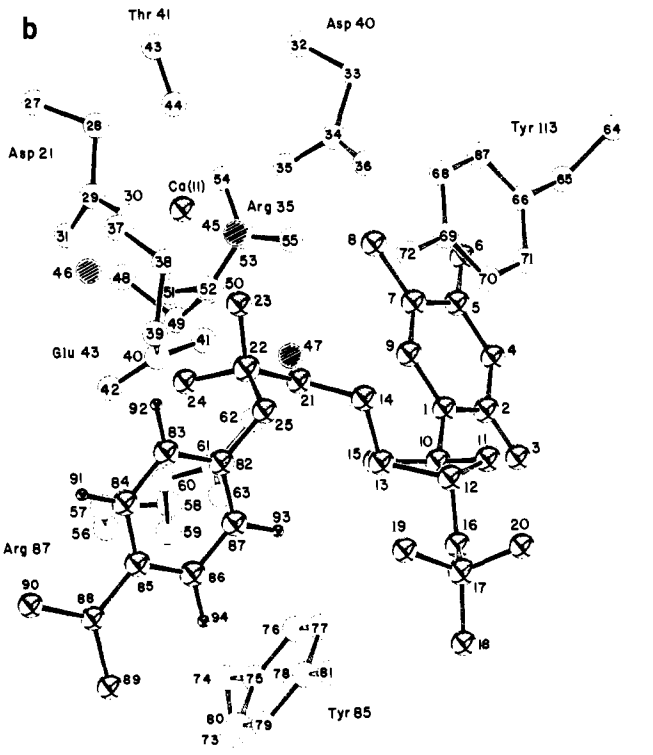

Figure 3. (a) Numbering scheme used for energy minimization of *p*-NO_2Ph-pdTp–Ca(II)–staphylococcal nuclease. For calculations on pdTp, the atoms corresponding to *p*-NO_2Ph were omitted. Since Thr-41 was away from the reaction zone, only the β C–O function was included. (b) ORTEP drawing of minimum energy conformation of *p*-NO_2Ph-pdTp–Ca(II)–staphylococcal nuclease. Numbers correspond to scheme shown in Figure 3a. Open circles designate atoms of the enzyme active site; shaded circles, atoms of the substrate. Filled circles are oxygen atoms of water molecules.

certainty in atomic position and to the choice of "strainless" bond parameters, can be minimized by slight changes in all atomic positions. For the set of coordinates selected, an initial strain energy of 780 kcal/mol was calculated. By a series of minimizations, designed in such a way that the basic conformation of the system was left unaltered and also that the α and β carbons

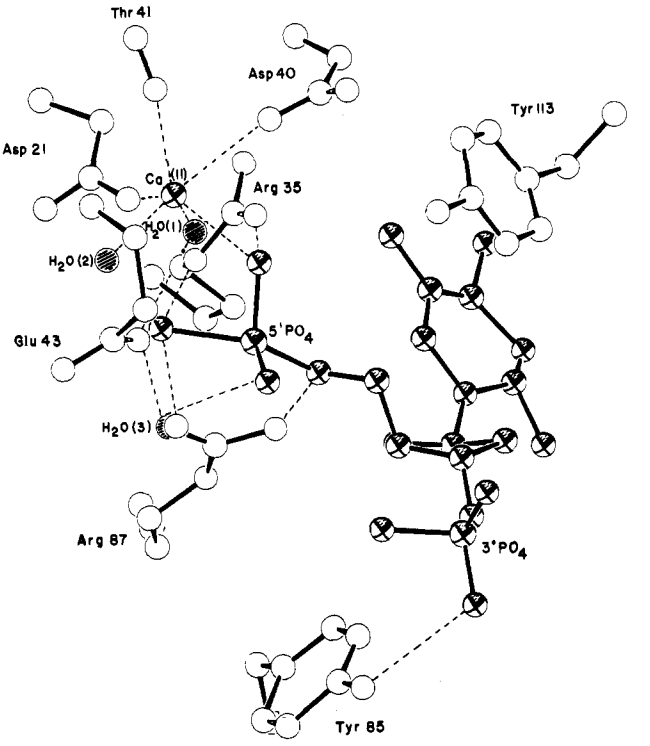

Figure 4. ORTEP drawing of pdTp in the enzyme active site of staphylococcal nuclease. Atom positions are obtained from 1.5-Å X-ray data.[13] Open circles designate atoms of the enzyme active site and shaded circles atoms of pdTp substrate. Filled circles indicate oxygen atoms of water molecules near the active site. Dotted lines indicate enzyme–substrate interactions.

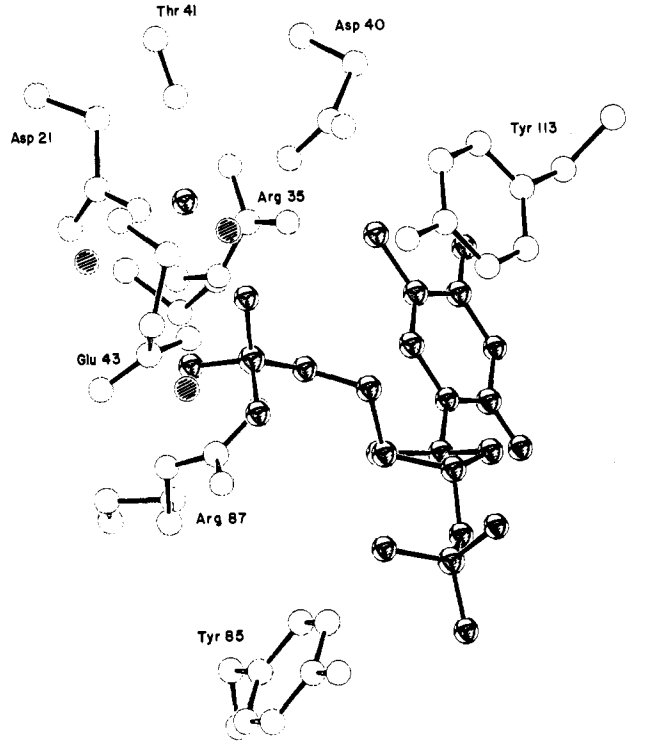

Figure 5. ORTEP drawing of pdTp in staphylococcal nuclease active site based on coordinates obtained from energy minimization. Open circles designate atoms of the enzyme; shaded circles, atoms of the pdTp substrate; filled circles, oxygen atoms of water molecules. Same orientation as Figure 3.

of the enzyme backbone were held in position, the strain energy was reduced to 1.2 kcal. This calculation is a two-step process which first brings the atom positions to better agreement with more conventional bond parameters for the substrate and then, owing

Table III. Enzyme-Substrate Interactions Included in Calculations

interaction	atom Nos.[a]	l_0 (Å)[c]	k_s[c] (mdyn/Å)	interatomic distance, Å: X-ray coordinates[b]	minimum energy coordinates: pdTp = substrate	minimum energy coordinates: p-NO_2Ph-pdTp = substrate
		Ca(II)-O Bonds[d]				
Ca-H_2O(1)	Ca_{26}-O_{45}	2.50	0.1	2.43	2.53	2.52
Ca-H_2O(2)	Ca_{26}-O_{46}	2.50	0.1	2.07	2.49	2.50
Ca-Thr-41	Ca_{26}-O_{44}	2.50	0.1	2.86	2.86	
Ca-Asp-21	Ca_{26}-O_{30}	2.50	0.1	2.28	2.46	2.43
Ca-Asp-40	Ca_{26}-O_{35}	2.50	0.1	2.72	2.44	2.45
Ca-5′-phosphate	Ca_{26}-O_{23}	2.50	0.1	2.64	2.64	2.60
		N-H···O Hydrogen Bonds				
Arg-35-5′-phosphate	N_{52}-O_{24}	2.90	0.1	3.19	2.90	2.92
Arg-35-5′-phosphate	N_{55}-O_{23}	2.90	0.1	1.96	2.90	2.90
Arg-87-5′-phosphate	N_{63}-O_{24}	2.90	0.1	3.18	2.90	2.90
Arg-87-5′-phosphate	N_{62}-O_{21}	2.90	0.1	2.57	2.91	2.91
		O-H···O Hydrogen Bonds				
Tyr-85-3′-phosphate	O_{81}-O_{18}	3.00	0.05	3.52	2.98	2.98
Glu-43-H_2O(1)	O_{41}-O_{45}	3.00	0.05	2.78	2.62	2.57
Glu-43-H_2O(3)	O_{41}-O_{47}	3.00	0.05	3.10	2.51	2.50
H_2O(3)-5′-phosphate	O_{47}-O_{25}	3.00	0.05	2.44	2.51	2.50

[a] See Figure 3 for numbering scheme. [b] Based on 1.5-Å X-ray data (ref 13) for pdTp-Ca(II) enzyme system. [c] The parameter l_0 is the "strainless" value for bond length; k_s is the stretching force for the bond. [d] Weak bending force constants were applied to give octahedral symmetry at the calcium ion.

to the introduction of the weak interactions shown in Table III, introduces small low-energy movements (generally rotational) of some residue atoms, particularly in the vicinity of the 5′-phosphate. These interactions, which seem reasonable to account for weak electrostatic and hydrogen bond interactions, provide a nonrigid environment and set the stage for the calculation of the hydrolysis pathway. In Table I a comparison is shown for the energy terms of the X-ray coordinates and of the minimized set for the system pdTp–Ca(II)–staphylococcal nuclease. In Table II, a comparison of various conformational parameters shows that the basic conformation of the substrate molecule was not altered in the energy minimization. The same point is shown graphically in the ORTEP drawings of Figures 4 and 5.

Conversion of pdTp to an Active-Substrate Complex. Since pdTp is an inhibitor of staphylococcal nuclease activity, it was necessary to modify the substrate to have a model of an active complex for hydrolysis reaction. The method used for this addition was the same as the method described in our previous paper.[7] The *p*-NO_2Ph group was added to the system, the torsional angle $O_{21}P_{22}O_{25}C_{82}$ was varied in 20° increments, and the structure was minimized at each increment. A conformation with a torsional angle $O_{21}P_{22}O_{25}C_{82}$ of 111° was selected as the lowest energy (−0.83 kcal/mol) of all the minimum energy structures resulting from the torsional angle rotation. Conformational parameters for the minimum energy configuration of *p*-NO_2Ph-pdTp–Ca(II)–staphylococcal nuclease are given in Table II, and an ORTEP drawing of the minimum energy structure is shown in Figure 3.

Enzyme-Substrate Interacations. Weak interactions between enzyme and substrate become extremely important in determination of substrate conformation and in the positioning of substrate for reaction. Table III gives the list of interactions included in the calculation, the specific pairs of atoms involved, "strainless" value of the bond length, the force constant between the two atoms, and the interatomic distance. The distances are calculated from the 1.5-Å X-ray coordinates[13] for the system pdTp–Ca(II)–enzyme and also for the minimum-energy coordinates for substrate–Ca(II)–enzyme where the substrate is pdTp or *p*-NO_2Ph-pdTp.

In general these interactions fall into two categories: hydrogen bonds and calcium–oxygen interactions. The hydrogen bonds include interactions between Arg-35 and Arg-87 with 5′-PO_4 and interaction of Tyr-85 with 3′-PO_4. These are similar to interactions included in our previous calculation.[7] However, in the 1.5-Å data, the region around the calcium ion appears quite changed as compared with the 2.0-Å data, requiring a different set of calcium–oxygen interactions and O–H–O hydrogen bond interactions involving one of the H_2O molecules, H_2O(3), near the active site. These interactions were included in all calculations and energy minimizations unless specific mention is made of their omission. The dashed lines in Figure 4 show all enzyme–substrate interactions. However, the calcium–oxygen interactions and the hydrogen bonds to H_2O(3) can be more clearly seen in a slightly different orientation as depicted in Figure 6.

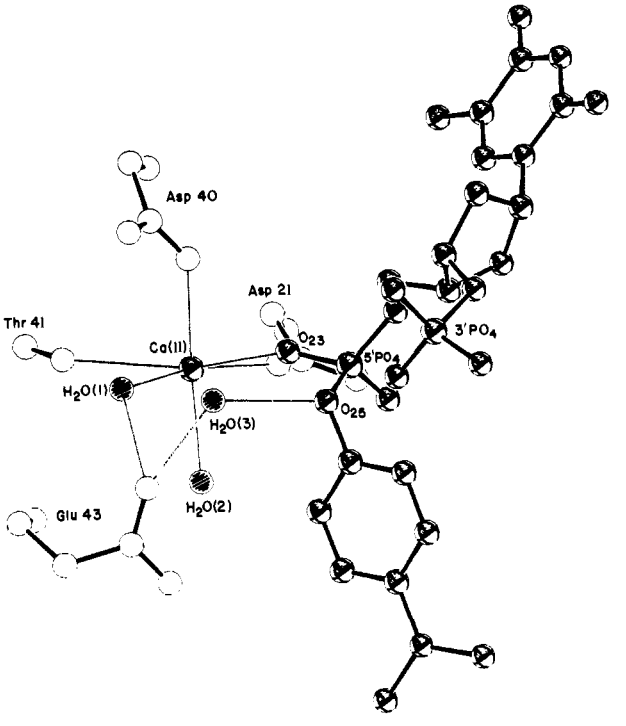

Figure 6. ORTEP drawing showing calcium coordination in *p*-NO_2Ph-pdTp–Ca(II)–enzyme system. Open circles indicate enzyme atoms; shaded circles, substrate; filled circles, oxygen atoms of water molecules. Weak interactions are shown by narrow bonds.

From Figure 6, one can visualize the proposed mechanism for action of staphylococcal nuclease.[3b] Nucleophilic attack by the water molecule bound to Glu-43 and an oxygen atom of the 5′-phosphate can occur in line with the P–O–R ester bond, where

Table IV. Bond Parameters for Attacking and Leaving Groups at Points along the Reaction Pathways

	points along the reaction pathways							
	1	2	3	4	5	6	7	8
P–OH bond[a]								
l_o[b]	3.00	2.50	2.00	1.90	1.80	1.78	1.70	1.60
k_s[c]	0.18	0.41	1.18	1.56	2.10	2.20	2.91	4.22
P–OR bond[d]								
l_o	1.60	1.61	1.67	1.71	1.77	1.78	1.92	3.00
k_s	4.22	3.99	3.22	2.84	2.30	2.20	1.49	0.18
sum of k_s	4.40	4.40	4.40	4.40	4.40	4.40	4.40	4.40

[a] P–OH bond is the P–O bond formed by attacking OH group. [b] l_o values are the "strainless" bond lengths (Å). [c] k_s values of the bond stretching force constants (mdyn/Å). [d] P–OR bond is the P–O bond of the leaving group.

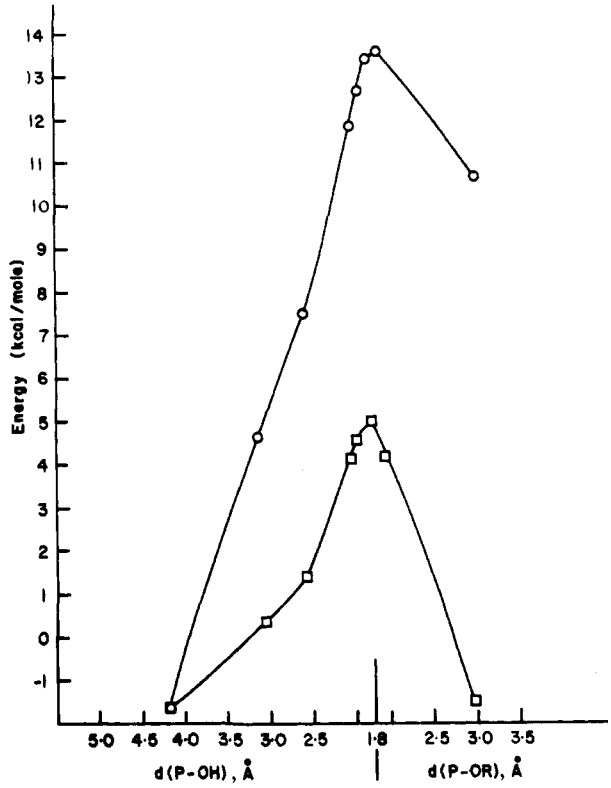

Figure 7. Energy profiles for two alternate modes of hydrolysis of *p*-NO_2Ph-pdTp in the staphylococcal nuclease environment. Circles indicate path 1; squares, path 2. See Figure 1 for definition of pathways. The attacking group is OH and leaving group is OR (R = *p*-NO_2Ph–O_{25} in path 1 and O_{21}–ribose in path 2. Experimentally, path 2 is the preferred path in enzymatic hydrolysis.

R = CH_2–ribose–base. The oxygen atom of the $H_2O(3)$ molecule is located about 3.5 Å from phosphorus. There is no force constant holding it at this distance.

Since the mechanism proposed by Cotton, Hazen, and Legg[3b] was based on electron density maps of pdTp–Ca(II)–nuclease, they were unable to ascertain the location of an additional R group attached to the 5′-phosphate. By the molecular mechanics minimization method, we have been able to show that the addition of a *p*-NO_2Ph group does not in any way diminish the feasibility of the proposed mechanism.

Hydrolysis Reaction Pathway. An energy profile was calculated for the hydrolysis of *p*-NO_2Ph–Ca(II)–nuclease by two different pathways as shown in Figure 1. The same conditions as described in our earlier paper[7] regarding phosphorus angles and force constants were imposed also in these calculations. It was necessary (1) to eliminate the force constants for two of the weak enzyme–substrate interactions involving $H_2O(3)$, the water molecule which provides hydroxide ion for nucleophilic attack; and (2) to add a hydrogen atom to O_{47}, the oxygen of $H_2O(3)$. For calculations of the energy profile along path 1, the attacking OH group was placed in line with *p*-NO_2Ph–O at a distance of 3.0 Å. For calculations along path 2, the attacking OH group was placed in

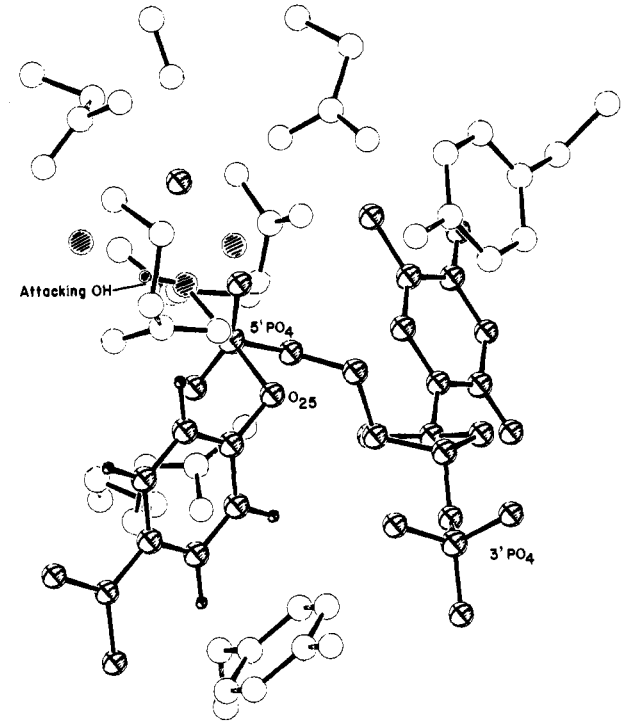

Figure 8. ORTEP drawing of path 1 transition state in hydrolysis of *p*-NO_2Ph-pdTp in the staphylococcal nuclease environment. Attacking OH is opposite O_{25}-Ph (see Figure 1). Phosphorus bond angles for the transition state are given in Table V, col. 6. Open circles designate atoms of enzyme, shaded circles, atoms of *p*-NO_2Ph-pdTp substrate; orientation of drawing is the same as Figure 3.

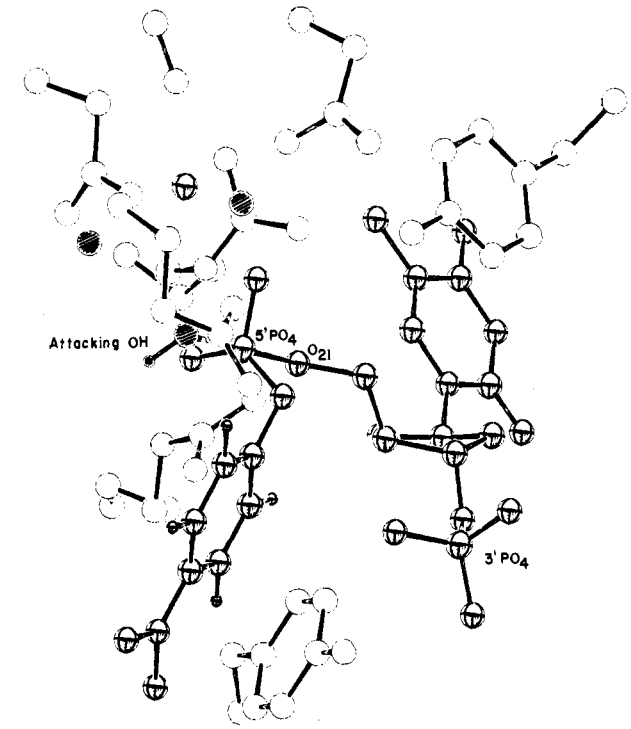

Figure 9. ORTEP drawing of path 2 transition state in hydrolysis of *p*-NO_2Ph-pdTp in the staphylococcal nuclease environment. Attacking OH is opposite O_{21}–ribose; see Figure 1. Phosphorus bond angles for the transition state are given in Table VI, col. 6. Open circles designate atoms of enzyme; shaded circles, atoms of *p*-NO_2Ph-pdTp substrate. Filled circles are oxygen atoms of water molecules; orientation of drawing is the same as Figure 3.

Table V. Reaction Path 1 for p-NO_2Ph-pdTp-Enzyme System[a]

point on pathway[b]	1	2	3	4	5	6[c]	7	8
bond length, Å								
P-OH	3.15	2.62	2.07	1.95	1.84	1.82	1.73	1.62
P-O_{21}	1.61	1.62	1.62	1.62	1.62	1.62	1.62	1.62
P-O_{23}	1.50	1.50	1.50	1.50	1.50	1.50	1.50	1.50
P-O_{24}	1.50	1.50	1.50	1.50	1.50	1.50	1.50	1.50
P-O_{25}	1.61	1.62	1.69	1.73	1.80	1.81	1.95	3.01
angles, deg								
O_{21}-P-O_{23}	123.3	121.3	116.3	115.5	115.0	114.8	115.4	115.0
O_{21}-P-O_{24}	92.6	91.0	88.4	87.9	87.4	87.4	87.0	87.0
O_{21}-P-O_{25}	89.3	88.1	86.6	86.0	85.2	85.0	83.6	73.9
O_{21}-P-OH	96.1	97.4	98.6	99.1	99.8	99.9	101.3	110.4
O_{23}-P-O_{24}	108.4	123.8	146.0	150.4	154.3	155.0	157.1	154.1
O_{23}-P-O_{25}	115.8	109.3	99.2	96.9	94.4	94.0	91.0	85.8
O_{23}-P-OH	61.8	68.3	78.7	81.1	83.6	84.1	87.1	93.0
O_{24}-P-O_{25}	125.2	116.9	105.5	102.9	100.1	99.6	96.8	87.7
O_{24}-P-OH	53.9	62.7	74.7	77.3	80.1	80.6	83.4	91.5
O_{25}-P-OH	174.6	174.5	174.8	174.9	175.0	175.0	175.1	175.6
energy (kcal/mol)								
ΣE_{str}	1.79	2.37	3.10	3.26	3.42	3.46	3.57	3.38
ΣE_{bend}	3.69	4.16	4.85	4.97	5.07	5.10	5.16	4.81
ΣE_{VDW}[d]	−0.78	0.97	3.84	4.39	4.84	4.95	4.69	2.38
$\Sigma E_{torsion}$	0.10	0.10	0.10	0.10	0.10	0.10	0.10	0.10
E_{steric} (total)	4.80	7.60	11.89	12.72	13.43	13.61	13.52	10.68

[a] Attacking group is OH; leaving groups is O_{25}. See Figure 3 for numbering scheme. [b] See Table IV. [c] Transition state. [d] $\Sigma E_{VDW} = \Sigma E_{NB} + \Sigma E_{EPR}$.

Table VI. Reaction Path 2 for p-NO_2Ph-pdTp-Enzyme System[a]

point on pathway[b]	1	2	3	4	5	6[c]	7	8
bond length, Å								
P-OH	3.04	2.57	2.06	1.95	1.84	1.82	1.73	1.61
P-O_{21}	1.61	1.63	1.70	1.74	1.81	1.82	1.97	2.99
P-O_{23}	1.50	1.50	1.50	1.50	1.50	1.50	1.50	1.50
P-O_{24}	1.50	1.50	1.50	1.50	1.50	1.50	1.50	1.50
P-O_{25}	1.60	1.60	1.60	1.60	1.61	1.61	1.60	1.60
angle, deg								
O_{21}-P-O_{23}	118.8	111.8	103.0	100.7	98.1	97.6	94.1	77.9
O_{21}-P-O_{24}	101.5	98.3	89.8	87.5	84.9	84.4	80.9	67.4
O_{21}-P-O_{25}	101.3	99.7	94.7	92.8	90.4	90.0	86.4	68.7
O_{21}-P-OH	179.0	178.8	179.2	179.3	179.4	179.4	179.6	179.8
O_{23}-P-O_{24}	103.7	107.0	110.3	110.6	110.8	110.7	110.9	107.5
O_{23}-P-O_{25}	105.6	108.9	113.3	114.1	114.5	114.6	114.6	102.3
O_{23}-P-OH	61.3	68.5	77.4	79.6	82.2	82.7	86.1	102.3
O_{24}-P-O_{25}	127.2	129.8	133.8	134.4	134.7	134.7	133.4	119.0
O_{24}-P-OH	77.5	80.6	89.4	91.8	94.6	95.1	98.7	112.5
O_{25}-P-OH	79.5	81.2	85.8	87.7	89.9	90.3	93.8	111.3
energy (kcal/mol)								
ΣE_{str}	0.80	1.02	1.45	1.50	1.52	1.54	1.35	0.57
ΣE_{bend}	2.84	2.85	2.90	2.89	2.86	2.86	2.74	2.41
ΣE_{VDW}[d]	−3.39	−2.58	−0.37	0.10	0.46	0.54	0.02	−3.52
$\Sigma E_{torsion}$	0.13	0.12	0.10	0.10	0.10	0.10	0.10	0.08
E_{steric} (total)	0.38	1.41	4.08	4.59	4.94	5.04	4.21	−0.46

[a] Attacking group is OH; leaving group is O_{21}. See Figure 3 for numbering scheme. [b] See Table IV. [c] Transition state. [d] $\Sigma E_{VDW} = \Sigma E_{NB} + \Sigma E_{EPR}$.

line with O-ribose at a distance of 3.0 Å. At several points along the reaction pathway, a minimum energy conformation was calculated after changing the values of the "strainless" bond lengths and force constants for the attacking and leaving groups, as given in Table IV. The transition state is the point where l_0(P–OH) = l_0(P–OR) = 1.78 Å (point 6). The condition was imposed, as described earlier,[7] that the sum of the two force constants for the attacking and leaving groups remain constant. All other parameters were set at the same values as used in the calculation of the minimum energy conformation of the p-Ph-pdTp–Ca(II)–nuclease system.

Results are listed in Tables V (path 1) and VI (path 2). The comparative energy profile is shown in Figure 7, and ORTEP drawings of the transition states for path 1 and path 2 are shown in Figures 8 and 9. From these results it can be seen that in the enzymatic environment path 2 is clearly the preferred pathway. This is the pathway which leads to products observed in enzymatic hydrolysis of p-NO_2Ph-pdTp.

Discussion of Mechanism

To compare these results with results for other systems, it seemed best to compare barrier heights along the reaction pathway. The height of the energy barrier is defined, for this purpose, as the difference between the energy of the transition state and the starting state for the reaction. Table VII shows energy barriers calculated for nonenzymatic and enzymatic systems.

To assess possible factors which caused the barrier height in path 1 to be so much greater than the barrier height in path 2 (1.5-Å data), several adjustments were made in the conditions imposed and the reaction pathway calculations were repeated; i.e., calcium ion was held fixed, the Ca–O_{23} force constant was removed, and hydrogen atoms were added at critical sites. From the results of these calculations two factors became obvious.

1. The barrier height for path 2 showed little or no variation (±0.5 kcal) in both the 2.0-Å and the 1.5-Å treatments, as well as in the nonenzymatic calculation. There seemed to be no obstruction to attack in line with O_{21}-ribose. The attacking OH could

Table VII. Calculated Energy Barriers[a] for Hydrolysis of p-NO_2Ph-pdTp (kcal/mol)

		enzyme environment	
	nonenzyme environment[b]	2.0-Å data[b]	1.5-Å data
path 1 $E_{trans\ state}$	17.94	8.81	13.61
$E_{initial}$	12.02[c]	1.53[c]	−0.83
$E_{barrier}$	5.92	7.28	14.44
path 2 $E_{trans\ state}$	18.12	6.70	5.04
$E_{initial}$	12.02[c]	1.53[c]	−0.83
$E_{barrier}$	6.10	5.17	5.87

[a] $E_{barrier}$ is the difference between energy of transition state and energy of initial configuration of p-NO_2Ph-pdTp. [b] Reference 7. The two pathways are of comparable energy in the absence of enzyme constraints. However, path 1 is the preferred path, consistent with observations, based on the better leaving group (p-NO_2Ph > thymidine 3'-phosphate), a factor not included in the present calculation. [c] Unpublished data.

move in unimpeded, and a transition state with approximate trigonal-bipyramidal symmetry could form with no major rearrangement of atoms.

2. The barrier height of path 1 in the enzymatic environment (based on the 1.5-Å data) was extremely sensitive to the calculation method employed. In fact, by manipulation of conditions imposed, it was possible to arrive at a transition state of somewhat lower energy, but to do so, one had to pass through an initial high energy barrier.

The calculations revealed that the high-energy barrier was due to the enzyme positioning of the Arg-35 residue with its nitrogen atom blocking the approach of the attacking OH in line with the p-nitrophenyl group. From the coordinates of the minimum energy conformation of p-NO_2Ph-pdTp–Ca(II)–enzyme (see Figure 3), it can be seen that the N_{52} atom (Arg-35) to phosphorus forms an angle of 180° with the P–O_{25} bond. The distance from N_{52} to phosphorus is 3.39 Å. Thus, as the OH approaches phosphorus, in line to O_{25}, extensive rearrangment of the system is required for the path 1 reaction in the enzymatic environment. This no doubt contributes to the unusual geometry at the transition state which has an O_{23}–P–O_{24} angle of 155° (Table V, point 6). Based on the nonrigid character of pentacoordinated phosphorus,[14] the program[12a] does not favor the trigonal bipyramid over the square pyramid; i.e., it allows for pseudorotation. The transition-state structure obtained for path 1 is best described as approaching a square pyramid which has O_{23}–P–O_{24} and O_{25}–P–OH as the trans basal angles.

These calculations expand the role of Arg–phosphate interactions. Cotton, Hazen, and Legg[3b] discussed their importance in neutralization of the phosphate charge and polarization of the phosphate group, thus enhancing the susceptibility of phosphorus to nucleophilic attack. From the results of the present calculations, Arg-35, in addition to its other functions, presumably has an even more specific role, i.e., blockage of the pathway that is most feasible in nonenzymatic hydrolysis.

In agreement with the mechanism outlined here, Mehdi and Gerlt[15] recently determined that staphylococcal nuclease hydrolyzes a stereoisomer of p-NO_2Ph-pdTp with inversion of configuration. However, they mention that the obseved inversion is also consistent with nucleophilic attack of Glu-43 on phosphorus if hydrolysis of the acyl phosphate ester intermediate occurs with C–O bond cleavage. Our preliminary probe of this mechanistic alternative shows the closest glutamate oxygen atom, O_{41}, to be out of range for effective nucleophilic attack. In the initial X-ray structure, the distance of O_{41} from phosphorus in pdTp is 5.35 Å and, in the minimized p-NO_2Ph-pdTp substrate, O_{41} is 5.22 Å from the phosphorus atom. Within our constraints, we find that as O_{41} of Glu-43 moves to 3.0 and 2.5 Å of phosphorus, the energy rapidly goes up, 9.4 and 21.0 kcal/mol, respectively. This compares with 0.4 and 1.4 kcal/mol for attack by $H_2O(3)$ under the same conditions (Table VI, points 1 and 2). Thus, unless the enzyme is unusually flexible, i.e., is able to allow Glu-43 to move rather freely, we believe glutamate attack is unlikely.

Acknowledgment. This investigation was supported by a grant from the National Institutes of Health (GM 21466) and is gratefully acknowledged. Appreciation is expressed to the University of Massachusetts Computing Center for generous allocation of computer time and to Dr. Jean R. Devillers, Paul Sabatier University, Toulouse, France, for his help in performing some of the calculations.

Registry No. p-NO_2Ph-pdTp, 24418-11-9.

(14) (a) Holmes, R. R. *ACS Monogr.* **1980**, No. 175. (b) Holmes, R. R. *Ibid.* No. 176. (c) Holmes, R. R. *Acc. Chem. Res.* **1979**, *12*, 257.
(15) Mehdi, S.; Gerlt, J. A. *J. Am. Chem. Soc.* **1982**, *104*, 3223.